High efficiency single Ag nanowire/p-GaN substrate Schottky junction-based ultraviolet light emitting diodes

Y. Wu,[1] T. Hasan,[2] X. Li,[1] P. Xu,[1] Y. Wang,[1] X. Shen,[1] X. Liu,[1] Q. Yang[1, a)]

[1]*State Key Laboratory of Modern Optical Instrumentation, Department of Optical Engineering, Zhejiang University, Hangzhou 310027, China*

[2]*Cambridge Graphene Centre, University of Cambridge, Cambridge CB3 0FA, UK*

Author to whom correspondence should be addressed. Electronic mail: qingyang@zju.edu.cn

Abstract:

We report a high efficiency single Ag nanowire (NW)/p-GaN substrate Schottky junction-based ultraviolet light emitting diode (UV-LED). The device demonstrates deep UV free exciton electroluminescence at 362.5 nm. The dominant emission, detectable at ultralow (<1 μA) forward current, does not exhibit any shifts when the forward current is increased. External quantum efficiency (EQE) as high as 0.9% is achieved at 25 μA current at room temperature. Experiments and simulation analysis show that devices fabricated with thinner Ag NWs have higher EQE. However, for very thin Ag NWs (diameter <250 nm), this trend breaks down due to heat accumulation in the NWs. Our simple device architecture offers a potentially cost-effective scheme to fabricate high efficiency Schottky junction-based UV-LEDs.

High efficiency ultraviolet light emitting diodes (UV-LEDs) are exploited in a wide range of applications, *e.g.* information storage, water purification, disinfection of medical tools, UV curing, phototherapy and medical diagnostics.[1-3] UV-LEDs with highest EQE (<10%, wavelength shorter than 365 nm) have been reported based on AlGaN and InGaAlN multiple-quantum-well (MQW) structures.[3] UV light sources have also been demonstrated using p-n homo-/heterojunctions[2,4] and metal-intrinsic layer-semiconductor (MIS) contacts.[5,6] However, to minimize the cost, more economical strategies to realize UV emitting devices are required. Schottky-type LEDs (ST-LEDs) based on metal-semiconductor (MS) contact are attractive for several reasons. First, ST-LEDs do not require complex processing such as those required for MQWs. Second, the device operation does not rely on p-n junction, reducing the difficulties associated with doping of semiconductors.[7] Finally, it does not require deliberate introduction of an intrinsic layer to reduce leakage current and to accumulate carriers near the interface, a key process in MIS LEDs.[5,8] On the other hand, ST-LED is cost-effective due to its simplistic materials and design requirement.[9,10] Nevertheless, the tradeoff is that the metal layer also absorbs a significant percentage of the LED output, resulting in severe deterioration of the device performance. Here, we propose an ST-LED based on a single Ag nanowire (NW)/p-GaN substrate Schottky junction. The Ag NW replacing the metal layer can significantly improve the compromised device performance due to its small footprint. Our LED exhibits free exciton emission centered at 362.5 nm under continuous operation with a maximum EQE of 0.9%. This efficiency is the highest reported value for UV-LEDs based on MS Schottky junction and is comparable to the UV-LEDs based on n- or p-type semiconductor nanowire/substrate hybrid structure[2,11]. Further experiments and simulation show that the EQE of the ST-LED increases with decreasing diameter of the Ag NW (d_{nw}) before accumulated heat effect overcomes the performance gain.

The schematic of the device, showing a single Ag NW across trenched substrates, is presented in Fig. 1(a). To fabricate the device, first, an Mg doped p-type GaN

substrate (Mg doping concentration ~1×10^{18} cm^{-3}) is epitaxially grown on sapphire by metalorganic chemical vapor deposition (MOCVD).[12] The next step involves cleaning and ethcing for the removal of the native oxide layer on the GaN substrate to form the Schottky junction. First, the GaN substrate is ultrasonically degreased using acetone, ethanol, and deionized (DI) water for 5 min each. The substrate is then treated with a buffered oxide etch (BOE) solution for 15 min. Finally, the GaN substrate is rinsed in DI water and dried in N_2. The p-electrodes are then fabricated by thermally evaporating Ni (20 nm)/Au (50 nm) onto GaN. An ITO (200 nm) coated sapphire substrate, used as the cathode, is placed closely beside the GaN substrate with a well-controlled gap (<35 μm) by micromanipulation under microscope. Ag NWs with d_{nw} ~120-500 nm and length >50 μm are synthesized by reducing silver nitrate ($AgNO_3$) with ethylene glycol (EG) in the presence of polyvinyl pyrrolidone (PVP) by a soft, self-seeding process.[13] The synthesized Ag NWs are purified via centrifugation in ethanol and then in deionized water for several cycles. The obtained suspension of Ag NWs is then deposited onto a clean glass substrate for subsequent manipulation. A single Ag NW is picked up from the glass substrate and transferred to the trenched substrates across the gap using a home-made fiber taper.[1] A scanning electron microscope (SEM) image of the device is shown in Fig. 1(b). The Ag NW is firmly attached to the substrate by van der Waals force.

The electrical measurements are carried out using an Agilent B1500 semiconductor analyzer. Electroluminescence (EL) properties of the ST-LED is measured using a fused silica fiber outfitted with a spectrometer calibrated by a power meter.[1] Since the total output power of a single NW LED is low, we use a purpose-built setup to measure the emission efficiency. For this, a 355 nm laser is input into the spectrometer and power meter to establish a linear relationship between the integrated spectrum and the measured power.[1] We use this relationship to calculate the output light power. All EL properties are measured under continuous device operation. The light collection efficiency of the EL measurement setup is ~2% (with a fiber N.A. of 0.22 and collecting light within a cone with 25.4^o apex angle,

giving an efficiency of ~2%). The photoluminescence (PL) spectrum is measured with the same setup using a frequency-tripled Nd:YAG pulsed laser (centered at 355 nm with 10 ns pulse width and 10 kHz repetition rate) as the excitation source. All the measurements are carried out at room temperature.

The current-voltage (I-V) characteristics of the device are presented in Fig. 2(a). A typical rectifying behavior is observed with a forward onset voltage at ~4.8 V. The linear curve in the inset for Ag NW on ITO reveals good Ohmic contact. Ni/Au also forms good Ohmic contact with p-GaN, as reported before.[1] Therefore, the diode-like rectification originates from the Ag NW/p-GaN Schottky junction. Fig. 2(b) shows room temperature EL of the device under different injection currents and the PL of p-GaN film. With our setup, EL signal can be obtained from the ST-LED at forward current as low as 500 nA. The spectra consist of strong UV emission and a weak defect-related[5] emission from 480 nm to 710 nm, with a maximum centered at ~570 nm. Two peaks constitute the UV luminescence: a dominant peak at 362.5 nm with ~7 nm full width at half maximum (FWHM) and a second peak, centered at 378.6 nm with ~30 nm FWHM. The 362.5 nm peak originates from the sharp, free exciton emission in GaN[14,15] while the second peak is assigned to isolated Mg acceptors in GaN.[14,15] The positions of both peaks, which originate from the essential characteristics of exciton-related transition in GaN,[15,16] are independent of forward current from 500 nA to 25 μA (Fig. 2(b), inset). We also investigate the statistical variation of the dominant peak position of 20 ST-LEDs (Fig. 2(c)). The devices show similar properties with a narrow emission distribution (~0.73 nm standard deviation).

A typical optical microscope image of the EL emission from the ST-LED is shown in Fig. 2(c) inset. The brighter regions along the Ag NW indicate that emissions come from the Schottky junction, where electrons from the Ag NW radiatively recombine with the holes in the p-GaN substrate. The dark regions along the Ag NW could be caused by local nonuniformities[17] (such as dislocations within the NW, variation in NW contact with the substrate *etc*) which block the electrons from being injected into GaN. Due to total reflection, not all the generated emission

can escape from the top of GaN, parts of the radiative emission are confined and propagate within the GaN film and subsequently emit at the edge of GaN (upper right in Figure 2(c) inset).

The integrated intensity of EL (L) versus current (I) (L-I curve) in Fig. 3(a) shows a superlinear dependence, indicating the co-existence of radiative and nonradiative process. The results can be fitted by the power law of $L \propto I^m$, where m accounts for the influence of nonradiative defects on the light emission characteristics.[18] The low exponent m=1.24 in our device suggests that radiative recombination increases at a faster rate than the nonradiative recombination, resulting in a small increase in EQE at higher forward current. The room temperature EQE of our ST-LED is estimated to be 0.9% at 25 μA forward current.

Table 1. Electroluminescence properties of different type LEDs based on simple structures.

Device Structure	Junction type	Peak wavelength (nm)	Onset current	EQE (%)	Ref.
ZnO NWs/p-GaN substrate	p-n	400-420	>1 mA	~2.5	11
n-GaN NW/p-GaN substrate	p-n	365	18 μA	Not reported	2
Graphene/SiO_2/p-GaN substrate	MIS	~400	~8 mA	Not reported	5
ITO/GaN:H/Au	Schottky	570	>5 mA	~10^{-4}	19
Au film/n-GaN substrate	Schottky	374	Not reported	<0.05	10,20
Ag NW/p-GaN substrate	Schottky	362.5	<1 μA	~0.9	This work

The EL characteristics of the ST-LEDs in our work are compared with LEDs in reported literature based on NW/thin film p-n junction, MIS junction and Schottky junction (Table 1). The EQE of our device is the highest reported to date for UV LEDs based on Schottky junction. We attribute the high efficiency to reduced extinction of emission due to the small diameter of Ag NW. The performance is also comparable to those of the UV-LEDs based on NW/thin film p-n hetero-/homojunctions and MIS junction, with a simpler device architecture and potentially, lower fabrication cost.

The dependence of device performance on d_{nw} is also investigated. Fig. 3(b) shows the relative EQE, derived by dividing the integrated EL intensity by the corresponding forward current of devices with d_{nw} ~170, 230, 250, 310, 450 and 470 nm, respectively. For d_{nw} >250 nm, the EQE increases with decreasing diameter. Indeed, EQE of ST-LED with d_{nw} ~250 nm is 2.5 times larger than that of 470 nm. An opposite trend is observed for d_{nw} <250 nm, with EQE at d_{nw} ~170 nm being only 70% of that measured at d_{nw} ~250 nm.

Interpretation of these experimental results is presented by analysing the carrier transportation and the emission distribution of the ST-LEDs. As shown in Fig. 4(a), under forward bias, electrons are directly injected from Ag NW into p-GaN and the recombination area is determined by the minority carrier diffusion length (L_n) and width of the space charge region (w).[7] For Mg doping level of ~10^{18} cm^{-3}, estimated L_n and w are ~1 μm and <60 nm, respectively.[21] Thus, L_n will dominate the recombination area and the active region (4-12 times larger than Ag NW radius) spreads into the p-GaN. Therefore, only a small part of the active region is covered (*e.g.* 12.5% is covered for the device with highest EQE at d_{nw} ~250 nm) in contrast to 100% if a metal layer[9,10] is used, improving the EQE.

Further investigation of the spatial distribution of the emission is computed by COMSOL. In our simulation, the emission from the recombination area is simplified to a plane wave of 362.5 nm wavelength with unity amplitude. It illuminates the Ag NW from the GaN substrate side. Fig. 4(b) presents the magnitude distribution of the

electric field of the emission. The Ag NW leaves a shadow behind it, where the field strength is reduced. We characterize the strength of the interaction by the scattering and absorption cross section, defined as $C_{sct} \equiv P_{sct} / I_0$, $C_{abs} \equiv P_{abs} / I_0$, respectively.[22] Here, I_0 is the intensity of an incident plane wave, P_{sct} and P_{abs} are the amount of power scattered or absorbed by the Ag NW, respectively. The calculated extinction cross section, defined as $C_{ext} \equiv C_{sct} + C_{abs}$, has a linearly decreasing trend with decreasing d_{nw}; see blue curve in Fig. 4(c). For instance, C_{ext} at d_{nw} ~250 nm is ~50% of that at 470 nm, which is consistent with the experimental results that EQE increases as d_{nw} decreases from 470 nm to 250 nm.

However, the trend in decreasing EQE for d_{nw} <250 nm is contrary to the simulation predictions. We attribute this discrepancy to heat effects. In our experiments, the ST-LEDs are under continuous operation, generating heat in the Schottky junction at room temperature.[9,19] We suggest that heat accumulation results in the decrease in measured EQE. Thermal analysis is performed using COMSOL to suppport this. Here, we consider a 3D model consisting of a single Ag NW across the GaN and ITO film on sapphire substrate under a constant heating source located at the interface of Ag NW and GaN. Thermal conductvity of 100 W/(m·K),[23,24] 8.2 W/(m·K),[25] 46 W/(m·K)[26] and 429 W/(m·K)[26] is used for GaN, ITO, Al_2O_3, and Ag bulk, respectively. Size-induced thermal conductivity decrease of NW is also considered in the simulation.[27,28] For the boundary condition, we set the ambient temperature to 293 K with a 5.0 W/(m^2·K) natural convection coefficient.[29] Fig. 4(d) shows the heat flux and temperature distribution of the ST-LED (d_{nw} =500 nm) at 200 μW heating power. The heat flux is represented by an arrow to indicate the direction. From the simulation results, the generated heat can be efficiently transferred by the Ag NW to the ITO substrate and surrounding air. However, with smaller d_{nw}, decreased thermal conductivity and cross sectional area leads to poor heat dissipation. The red curve in Fig. 4(c) shows the junction temperature increase from 308 K to 344 K when d_{nw} decrease from 500 nm to 100 nm. Previous reports have pointed out that

EQE exponentially decreases with increasing temperature due to less confinement of carriers[30, 31] and increased nonradiative processes such as Auger,[32] Shockley–Read–Hall recombination.[33] We therefore suggest that the increase in temperature compromises the performance enhancement of our ST-LEDs, leading into an optimum diameter (*e.g.*~250 nm in our experiments) of Ag NW for device fabrication.

In conclusion, we demonstrate a ST-LED architecture based on single Ag NW/p-GaN substrate Schottky junction. The emission from the ST-LED is dominated by free exciton emission at 362.5 nm with low defects-related emission. By taking advantage of the nanosized Schottky junction, we achieve EQE as high as 0.9% at 25 μA forward current at room temperture. Also, EL can be detected at low current levels (~500 nA). Further investigation shows that Ag NW with smaller diameter can improve the performance of the ST-LEDs. However, this observation is valid for d_{nw} >250 nm, below which heat accumulation within the NW compromises the device EQE. Owing to the high EQE, our simple device architecture has the potential to be a cost effective alternative to traditional UV-LEDs and can also be integrated into nano-optoelectronic systems.

This work is supported by National Key Basic Research Program of China (No. 2013CB328703), National Natural Science Foundation of China (No. 51372220 and 61177062). TH acknowledges funding from the Royal Academy of Engineering (Graphlex).

[1] Q. Yang, W. H. Wang, S. Xu, and Z. L. Wang, Nano Lett. **11**, 4012 (2011).

[2] A. Motayed, A. V. Davydov, M. He, S. N. Mohammad, and J. Melngailis, Appl. Phys. Lett. **90**,183120 (2007).

[3] M. Kneissl, T. Kolbe, C. Chua, V. Kueller, N. Lobo, J. Stellmach, A. Knauer, H. Rodriguez, S.Einfeldt, Z. Yang, N. M. Johnson, and M. Weyers, Semicond. Sci. Technol. **26**, 014036 (2011).

[4] X. Li, J. J. Qi, Q. Zhang, Q. Wang, F. Yi, Z. Z. Wang, and Y. Zhang, Appl. Phys. Lett. **102**, 221103 (2013).

[5] C. W. Chang, W. C. Tan, M. L. Lu, T. C. Pan, Y. J. Yang, and Y. F. Chen, Adv. Funct. Mater. **23**, 4043 (2013).

[6] X. Y. Liu, C. X. Shan, S. P. Wang, H. F. Zhao, and D. Z. Shen, Nanoscale **5**, 7746 (2013).

[7] S. Chu, G. Wang, W. Zhou, Y. Lin, L. Chernyak, J. Zhao, J. Kong, L. Li, J. Ren, and J. Liu, Nat. Nanotechnol. **6**, 506 (2011).

[8] B P. Chen, X. Y. Ma, and D. R. Yang, Appl. Phys. Lett. **89**, 111112 (2006).

[9] T. Honda, T. Kobayashi, S. Komiyama, and Y. Mashiyama, J. Vac. Sci. Technol. B **25**, 1529 (2007).

[10] T. Honda, N. Sakai, S. Komiyama, M. Hayashi, and T. Igaki, Phys. Status Solidi C **9**, 778 (2012).

[11] S. Xu, C. Xu, Y. Liu, Y. F. Hu, R. S. Yang, Q. Yang, J. H. Ryou, H. J. Kim, Z. Lochner, S. Choi, R. Dupuis, and Z. L. Wang, Adv. Mater. **22**, 4749 (2010).

[12] Y. Zhang, S. C. Shen, H. J. Kim, S. Choi, J. H. Ryou, R. D. Dupuis, and B. Narayan, Appl. Phys. Lett. **94**, 221109 (2009).

[13] Y. G. Sun, Y. D. Yin, B. T. Mayers, T. Herricks, and Y. N. Xia, Chem. Mater. **14**, 4736 (2002).

[14] U. Kaufmann, M. Kunzer, H. Obloh, M. Maier, C. Manz, A. Ramakrishnan, and B. Santic, Phys. Rev. B **59**, 5561 (1999).

[15] U. Kaufmann, M. Kunzer, M. Maier, H. Obloh, A. Ramakrishnan, B. Santic, and P. Schlotter, Appl. Phys. Lett. **72**, 1326 (1998).

[16] D. C. Reynolds, D. C. Look, and B. Jogai, J. Appl. Phys. **88**, 5760 (2000).

[17] J. Bao, M. A. Zimmler, F. Capasso, X. Wang, and Z. F. Ren, Nano Lett. **6**, 1719 (2006).

[18] J. J. Dong, X. W. Zhang, Z. G. Yin, J. X. Wang, S. G. Zhang, F. T. Si, H. L. Gao, and X. Liu, Appl. Phys. Lett. **100**, 171109 (2012).

[19] S. Yagi, S. Suzuki, and T. Iwanaga, Jpn. J. Appl. Phys. Part 2-Lett. **40**, L1349

(2001).

[20] T. Kobayashi, S. Egawa, M. Sawada, and T. Honda, Phys. Status Solidi C **4**, 61 (2007).

[21] K. Kumakura, T. Makimoto, N. Kobayashi, T. Hashizume, T. Fukui, and H. Hasegawa, Appl. Phys. Lett. **86**, 052105 (2005).

[22] Z. C. Ruan and S. H. Fan, Phys. Rev. Lett. **105**, 013901 (2010).

[23] Z. H. Su and J. A. Malen, ECS Trans., **58**, 343 (2013).

[24] B. C. Daly, H. J. Maris, A. V. Nurmikko, M. Kuball and J. Han, J. Appl. Phys. **72**, 3820 (2002).

[25] H. K. Lee and J. S. Yu, Semicond. Sci. Technol. **26**, 095006 (2011).

[26] T. L. Bergmanf, A. S. Lavine, F. P. Incropera, and D. P. Dewitt, Fundamentals of Heat and Mass Transfer, 7th ed. (Wiley, New York, 2011).

[27] T. Tritt, Thermal Conductivity: Theory, Properties, and Applications (Kluwer Academic/Plenum, New York, 2004).

[28] F. Volklein, H. Reith, T. W. Cornelius, M. Rauber, and R. Neumann, Nanotechnology **20**, 325706 (2009).

[29] L. Yang, D. X. Dai, and S. L. He, Opt. Commun. **281**, 2467 (2008).

[30] C. Huh, W. J. Schaff, L. F. Eastman, and S. J. Park, IEEE Electron Device Lett. **25**, 61 (2004).

[31] J. Senawiratne, A. Chatterjee, T. Detchprohm, W. Zhao, Y. Li, M. Zhu, Y. Xia, X. Li, J. Plawsky, and C. Wetzel, Thin Solid Films **518**, 1732 (2010).

[32] E. Kioupakis, P. Rinke, K. T. Delaney, and C. G. Van de Walle, Appl. Phys. Lett. **98**, 161107 (2011).

[33] H. P. Nguyen, K. Cui, S. Zhang, M. Djavid, A. Korinek, G. A. Botton, and Z. Mi, Nano Lett. **12**, 1317 (2012).

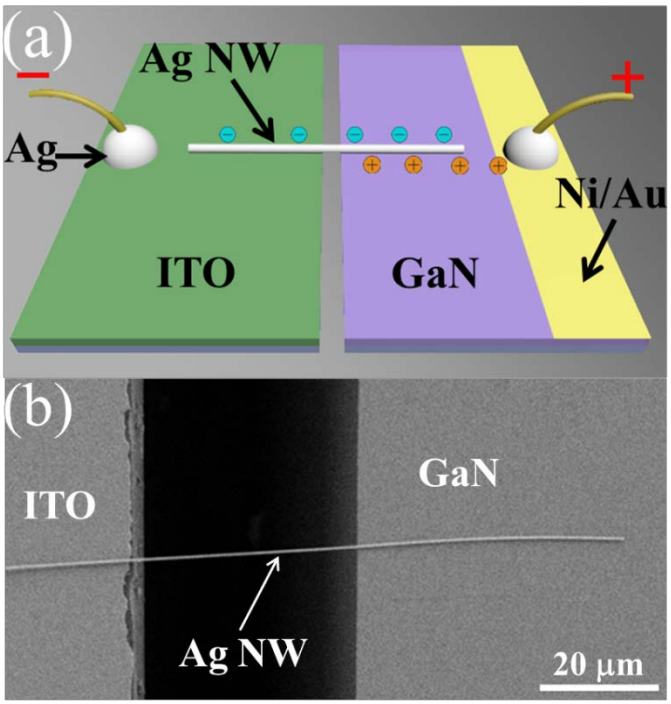

FIG. 1. (a) Schematic of the single Ag NW/p-GaN ST-LED. (b) SEM image of the as-fabricated device.

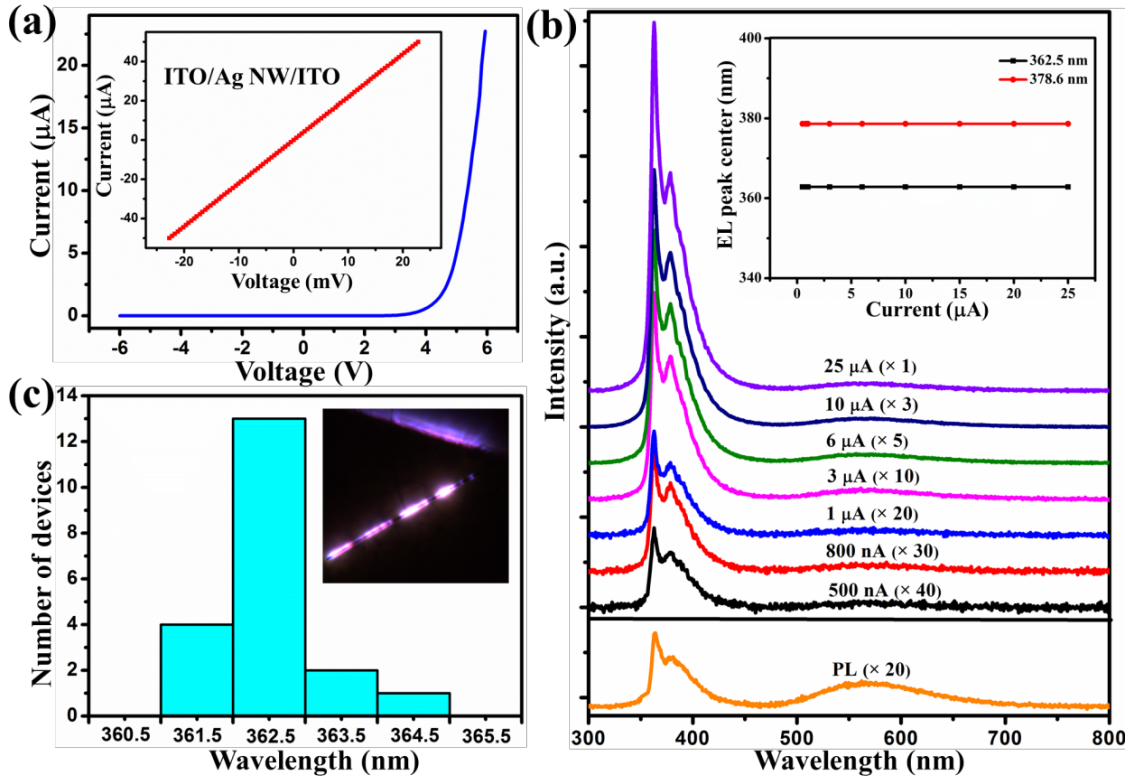

FIG. 2. (a) I-V characteristics of the as-fabricated device. The inset shows Ohmic contact behavior of the ITO/Ag NW/ITO structure. (b) EL spectra of the device under injection currents from 500 nA to 25 μA and the PL spectrum of p-GaN under 355 nm pulsed laser excitation. Inset: The EL peak position (362.5 nm and 378.6 nm) versus different forward currents of the same device. (c) The dominant emission peak distribution of 20 devices. Inset: a typical optical microscope image of the emission of the ST-LED.

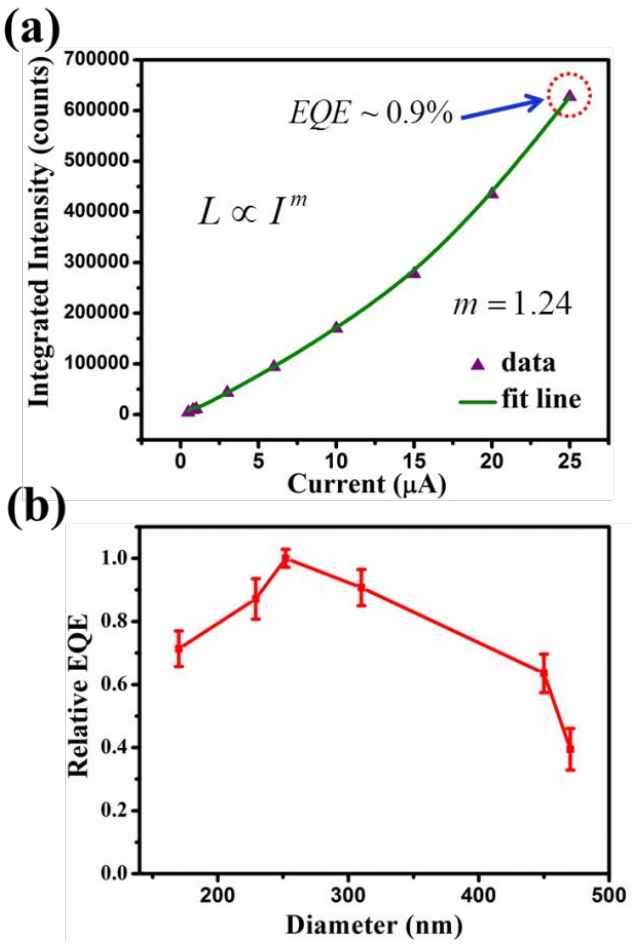

FIG. 3. (a) Integrated EL intensities as a function of the injection current. The solid line represents the fitting result based on the power law $L \propto I^m$.(b) Relative EQE of ST-LEDs fabricated with Ag NWs of different diameters.

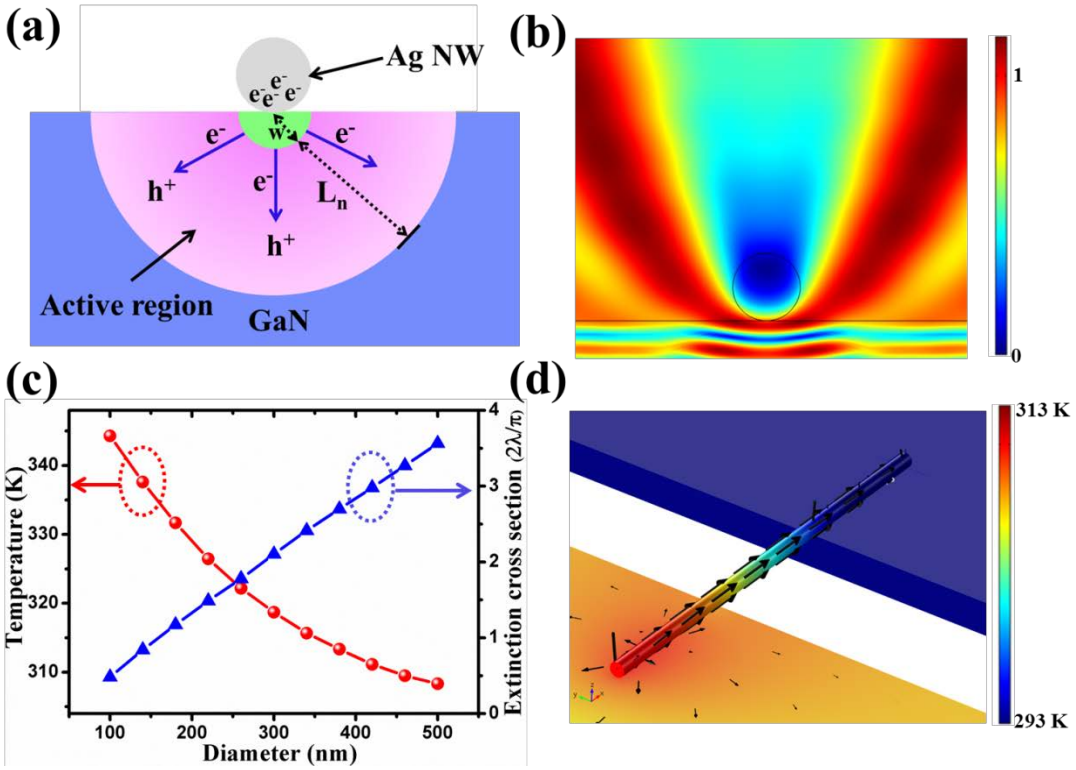

FIG. 4. (a) Active region diagram of the ST-LED. The size of the region is defined by the sum of space charge region and diffusion length ($w+L_n$). (b) Calculated electric field distribution $(E_x^{\,2}+E_y^{\,2}+E_z^{\,2})^{1/2}$ of emitted light. The diameter of Ag NW used here is 180 nm. (c) Extinction cross section of Ag NW (blue curve) and temperature of the Schottky junction (red curve) as a function of d_{nw}. (d) Heat flux and temperature distribution of the ST-LED (heating power 200 μW, d_{nw} =500 nm. Normally, the device is operated at 5-10 V, the current is about 15-30 μA).